

51

N92-293707  
704982  
P-17

# Geometric Distortion Analysis of a Wide-Field Astrograph

W. M. Owen, Jr.  
Navigation Systems Section

S. B. Shaklan  
Optical Sciences and Applications Section

*Ground-based optical navigation seeks to determine the angular position of a star, Solar System body, or laser-emitting spacecraft relative to objects with well-known coordinates. Measurement accuracies of 25 nrad would make optical techniques competitive with current radio metric technology. This article examines a proposed design for a wide-field astrograph and concludes that the deviation of an image centroid from the ideal projection can be modeled to the desired accuracy provided that the field of view does not exceed 5 deg on a side.*

## I. Introduction

Astrometry, the science of measuring angular positions of celestial objects, is currently in renaissance thanks to new instrumentation such as the Multichannel Astrometric Photometer [1], the Hipparcos spacecraft [2], and the Mark III stellar interferometer [3]. These devices, whether orbiting or ground-based, have increased the precision of an angular measurement by two orders of magnitude compared to conventional photographic or transit-circle techniques.

Optical angular measurements accurate to 25 nrad (5 mas) could revolutionize JPL's spacecraft navigation as well. Ground-based observations of asteroid 951 Gaspra, while good to only 0.1 arcsec, nevertheless contributed greatly<sup>1</sup> to the successful flyby of that asteroid by Galileo

in 1991. Measurements of the satellites of Jupiter and of Saturn could provide accurate ephemerides of these objects, thereby improving the power of onboard navigation images taken by the Galileo or Cassini spacecraft. And direct optical measurements of the laser light emitted by a future spacecraft can determine its trajectory position relative to its target.

One of the tasks necessary in defining a future optical navigation system is to assess the capability of various instruments to deliver relative positions at the 5-mas (25-nrad) level<sup>2</sup> over a relatively wide (5- or 6-deg) field of view. The instrument itself must perform at that level; the problem of measuring images in the focal plane is a separate issue.

This article reports on the optical characteristics of one candidate, a proposed wide-field astrograph designed by the United States Naval Observatory. This instrument

<sup>1</sup> D. K. Yeomans and M. S. Keesey, "Updated Orbit and Ephemeris for Asteroid 951 Gaspra," JPL Interoffice Memorandum 314.6-1332 (internal document), Jet Propulsion Laboratory, Pasadena, California, August 30, 1991. More detailed accounts of the Gaspra encounter navigation will be presented at the AIAA/AAS Astrodynamics Conference in Hilton Head, South Carolina, in August 1992.

<sup>2</sup> G. Null, "Wide-Field Telescope Selection Results," JPL Interoffice Memorandum 314.8-815 (internal document), Jet Propulsion Laboratory, Pasadena, California, December 4, 1991.

has a clear aperture of 36 cm, a focal length of 3.6 m, a plate scale of 57.3 arcsec/mm, and a 6-deg field of view; the focal length in particular is similar to those of the 51-cm astrographs at Lick Observatory and Yale University Observatory.

Analysis of this instrument involved simulating stellar images at various places in the focal plane, finding the centroids of each image, and developing a model to account for systematic differences between the observed positions of these centroids and their ideal positions as predicted by a pinhole projection. The observed centroids can deviate from the ideal projection by almost 0.4 arcsec, necessitating the use of higher order terms in the transformation model. However, most of the deviation can be accommodated by one third-degree radial term, and the remainder is on the order of 2–7 mas.

The authors conclude that the instrument under consideration will indeed be suitable for 5-mas astrometry over a 5-deg  $\times$  5-deg field of view.

## II. Image Generation

The Controlled Optics Modeling Package (COMP) was used to simulate images in the focal plane, at steps of 0.5 deg (roughly 31 mm) from  $-3$  deg to  $+3$  deg in both  $x$  and  $y$ . The symmetry of the problem allowed generation of only those 28 images in the first quadrant for which  $x \geq y$ , marked by the filled dots in Fig. 1; the others follow from these. A total of  $13^2 = 169$  image points was therefore effectively obtained.

The COMP program contains both ray trace and diffraction analysis capabilities. The advantages of this program are that it can automatically calculate highly aberrated or off-axis diffraction patterns while providing direct access to optical parameters for modification and sensitivity testing. COMP is not a design tool, but an analysis subroutine that can automatically generate sets of images or sensitivity tables.

For this astrograph study, 902 rays were traced through the system to produce each image. The rays were traced to the focal plane, then back-propagated to the exit pupil onto a spherical reference surface whose center of curvature was defined by the intersection of the chief ray and the focal plane. The spherical phase term was removed, and a Fourier transform was performed in order to calculate a monochromatic image. The image was stored as a  $100 \times 100$  array of brightness values, with each number representing the intensity within a  $1\text{-}\mu\text{m}$  square in

the focal plane. Subsequent wavelengths were treated in the same fashion, except that the reference sphere was always centered on the same point as the first one. The five monochromatic images (at  $\lambda = 705.6, 650.0, 610.0, 587.6,$  and  $546.0$  nm) for each source position were then coadded to produce the final image files.

Images formed by the astrograph are diffraction limited on-axis, and show a slight coma at 3 deg off-axis. The first Airy ring is not broken, indicating weak aberration. Chromatic aberration was negligible.

One important question is to determine how much distortion is introduced by the finite number of rays, the finite number of Fourier grid points, the stepwise change in aperture representation due to vignetting, and pixellation effects in the image plane. One metric of the amplitude of these effects is to compare the ray centroids to diffraction centroids. One finds that diffraction centroids are within 0.8 mas of ray centroids throughout the field, which is well within the accuracy required for this study. A second metric is simply to increase the number of rays and grid points. Again, the distortion did not significantly change.

A second question involves the accuracy of the polychromatic approximation in this modeling. Because only five wavelengths were used to simulate a broad band, the composite Airy pattern is not a true representation of the broadband image. However, an empirical study showed that the major difference occurred only near the first and second ring minima. Because the images remain highly symmetric throughout the field, the small error does not significantly shift the centroids. Further, the ring minima regions are not particularly important in image centroiding.

## III. Image Centroiding

Image centroids for each image file were determined by using a data number (DN) filter. Each image is modeled as the sum of a point-spread function (PSF) and a constant background; the PSF itself is smoothed from a square array of brightness values. The coordinates of the center of the PSF, the amplitude of the PSF, and the background level are the unknowns in an iterated linear least-square process. The on-axis image was used as the PSF for all images. The brightness values (DN's) in each pixel of an image form the observation set. The variance in the DN in each pixel was composed of two parts: a constant to represent read noise, and a part proportional to the DN level itself to represent photon statistics. The resulting

centroids carry a formal error of  $\pm 0.025 \mu\text{m}$  in the focal plane (1.4 mas on the sky). The centroids were first computed in pixel and line coordinates within each image file, then transformed into millimeter coordinates in the focal plane.

#### IV. Plate Constants

Given the image centroids determined above and the ideal coordinates of each image, one seeks a transformation from measured to ideal coordinates. Following [4] or [5], denote the measured coordinates by  $(x, y)$  and the ideal coordinates by  $(\xi, \eta)$ . Model the transformation as a polynomial in each coordinate:

$$\xi = \sum_i \sum_j a_{ij} x^i y^j$$

and similarly for  $\eta$ . The two coordinates are handled independently, and symmetry allows one to examine only  $\xi$ . The  $a_{ij}$  are the solution parameters (the plate constants, for in classical astrometry these are found for each photographic plate from reference star images on that plate). The best model is generally considered to be the one with the fewest parameters such that the fit is acceptable.

From symmetry, any displacement of an image centroid from its ideal location must be in the radial direction, as in this analysis all the astrograph lenses were perfectly aligned. Aberration theory in geometrical optics also dictates that the displacement must be proportional to an odd power of the separation  $r$  of the image from the optical axis. Thus, the leading nonlinear term in  $x$  is  $xr^2$ , which is represented in the plate model by the two coefficients  $a_{30}$  and  $a_{12}$ . Trial solutions confirmed that the only nonzero terms in the plate model were those with  $i$  odd and  $j$  even. Accordingly, one can construct a more restrictive model,

$$\xi = \sum_k b_k r^{2k} x$$

in which the only displacements allowed were proportional to odd powers of  $r$ .

Table 1 gives coefficients for various solutions: those in terms of  $a_{ij}$  on the top, and those in terms of  $b_k$  at the bottom. Each of the maximum degree numbers represents the highest degree of the solution; this is the largest value

of  $(i + j)$  or  $(2k + 1)$  as appropriate. The formal errors of the coefficients are at most 1 in the final digit shown.

Table 2 summarizes the post-fit residuals for each case. The residuals generally reach a maximum in the corners of the field, but there is a secondary maximum not far from the origin. The table gives these values as well as the rms residual for all 169 images.

It is evident that low-order fits do not model the actual image centroid locations well in the corners of the full 6-deg  $\times$  6-deg field. The analysis was therefore repeated using only a 5-deg  $\times$  5-deg field by omitting the first and last row and column of images. The results appear in Tables 3 and 4. Now a third-degree fit meets the 5-mas requirement even in the corners of the field.

#### V. Conclusions and Discussion

The ideal projection is obviously not sufficient for a full 6-deg  $\times$  6-deg field, as distortions in this instrument reach 0.385 arcsec (in each coordinate) in the corners of the field. A third-degree fit removes most of the distortion, leaving residuals on the order of 2–7 mas or 10–35 nrad. In order to achieve the design goal of 25 nrad, it will be necessary to include the fifth-degree term or else to restrict the field of view to 5-deg square.

It is clear from the size of the residuals (Table 2) that it should be sufficient to model the astrograph by

$$\xi = b_0 x + b_1 r^2 x + b_2 r^4 x$$

the full generality of the  $a_{ij}$  should not be necessary. This is true, however, only if the optics are perfectly aligned. Any one of the five lenses can move in any direction by up to  $8 \mu\text{m}$  without introducing more than 5 mas of additional aberration.<sup>3</sup> Random motions of this size are not likely (except for thermal expansion), as the lenses would be rigidly mounted in a cell. However, it is not at all clear that the assembly process can be controlled to that tolerance. Although one can expect stability, one should also expect the instrument to be misaligned, and these inevitable misalignments will modify the radial distortion pattern of the perfectly aligned system. Accordingly, the

<sup>3</sup> S. Shaklan and J. Yu, "Images Formed With 36-cm Astrograph: Results to Supersede OSAS DFM 91-166," JPL Interoffice Memorandum OSAS DFM 91-173 (internal document), Jet Propulsion Laboratory, Pasadena, California, November 8, 1991.

full model in terms of  $a_{ij}$  should be employed if the instrument is built.

In practice, most astrometrists are loath to include terms higher than third degree in their plate solutions, simply because most star fields do not contain enough reference stars to support the higher terms. Also, as mentioned above, in most cases the plate constants are determined independently for each plate, because non-instrumental effects such as atmospheric refraction and dispersion will randomly corrupt the instrumental distortions. These real-world considerations do not invalidate this study. Rather, the instrumental distortion model should be found by testing the optics in the laboratory, and the model parameters and their covariance used as a priori information when reducing actual observations.

Outside the scope of this article is the requirement to measure image location to the 5-mas level. For this instrument, this requirement translates into a measurement precision (and accuracy) of about  $0.1 \mu\text{m}$ . Maintaining this accuracy over a region nearly 40 cm on a side may be challenging.

In conclusion, the candidate astrograph design suffers from radial distortion but that can be modeled with one parameter provided that the field of view is 5 deg on a side. Including terms to fifth degree will produce a model good to 1 mas and will allow the use of a 6-deg field, but the coefficients may be difficult to determine in practice. The instrument design is therefore viable provided that detectors can be found to exploit its excellent optical qualities.

## Acknowledgment

The work of Jeffrey Yu to help create the image files for this analysis is gratefully acknowledged.

## References

- [1] G. D. Gatewood, "The Multichannel Astrometric Photometer and Atmospheric Limitations in the Measurement of Relative Positions," *Astron. J.*, vol. 94, no. 1, pp. 213-224, July 1987.
- [2] M. A. C. Perryman et al., *The Hipparcos Satellite*, European Space Agency, Publication SP-1111, vols. I-III, Paris, France, June 1989.
- [3] M. Shao, M. M. Colavita, B. E. Hines, D. H. Staelin, D. J. Hutter, K. J. Johnston, D. Mozurkewich, R. S. Simon, J. L. Hershey, J. A. Hughes, and G. H. Kaplan, "The Mark III Stellar Interferometer," *Astron. Astrophys.*, vol. 193, pp. 357-371, 1988.
- [4] A. König, "Astronomy with Astrographs," in *Astronomical Techniques: Vol. 2, Stars and Stellar Systems*, edited by A. Hiltner, Chicago: University of Chicago Press, pp. 461-486, 1962.
- [5] H. Eichhorn, *Astronomy of Star Positions*, New York: Frederick Ungar Publishing Co., pp. 68-76, 1974.

**Table 1. Solution parameters for 6-deg field.**

Parameter	Maximum degree			
	1	3	5	7
$a_{10}$	0.9999655948	1.000008736	1.000009976	1.000010197
$a_{30}$		-0.0011189094	-0.0011969770	-0.0012239529
$a_{12}$		-0.0011063839	-0.0011871044	-0.0012123322
$a_{50}$			0.0011528	0.002152
$a_{32}$			0.0018920	0.003283
$a_{14}$			0.0009628	0.001705
$a_{70}$				-0.0117
$a_{25}$				-0.0196
$a_{34}$				-0.0147
$a_{16}$				-0.0070
$b_0$	0.9999655948	1.000008630	1.000009925	1.000010154
$b_1$		-0.0011116554	-0.0011895162	-0.001214510
$b_2$			0.00097727	0.0017079
$b_3$				-0.00615

**Table 2. Residual statistics for 6-deg field.**

Using $a_{ij}$	Maximum degree			
	1	3	5	7
RMS residual, $\mu\text{m}$	2.1277	0.0349	0.0043	0.0021
RMS residual, mas	121.91	2.00	0.25	0.12
Worst central residual, $\mu\text{m}$	3.233	0.073	0.014	0.007
Worst central residual, mas	185.2	4.2	0.8	0.4
Worst corner residual, $\mu\text{m}$	6.720	0.118	0.009	0.003
Worst corner residual, mas	385.0	6.8	0.5	0.2
Using $b_k$	Maximum degree			
	1	3	5	7
RMS residual, $\mu\text{m}$	2.1277	0.0369	0.0050	0.0027
RMS residual, mas	121.91	2.11	0.28	0.15
Worst central residual, $\mu\text{m}$	3.233	0.078	0.015	0.009
Worst central residual, mas	185.2	4.5	0.9	0.5
Worst corner residual, $\mu\text{m}$	6.720	0.125	0.010	0.004
Worst corner residual, mas	385.0	7.2	0.6	0.2

**Table 3. Solution parameters for 5-deg field.**

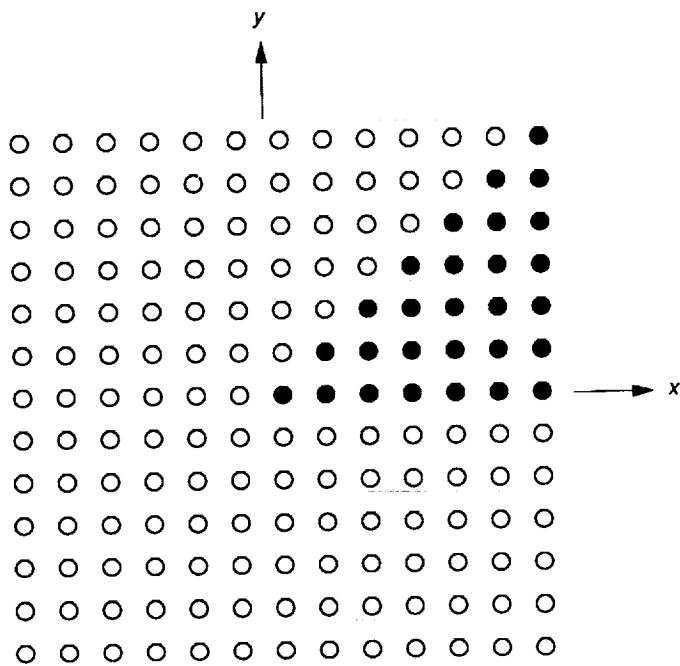
Using $a_{ij}$	Maximum degree			
	1	3	5	7
$a_{10}$	0.9999779128	1.000009343	1.000010126	1.000010264
$a_{30}$		-0.0011415289	-0.001211976	-0.00122835
$a_{12}$		-0.0011294587	-0.001200062	-0.00122944
$a_{50}$			0.0014983	0.001925
$a_{32}$			0.0023167	0.004635
$a_{14}$			0.0011932	0.002338
$a_{70}$				0.00
$a_{25}$				-0.04
$a_{34}$				-0.04
$a_{16}$				-0.01
$b_0$	0.9999779128	1.000009268	1.000010085	1.000010271
$b_1$		-0.0011344615	-0.0012033140	-0.001232187
$b_2$			0.00121582	0.002412
$b_3$				-0.0143

**Table 4. Residual statistics for 5-deg field.**

Using $a_{ij}$	Maximum degree			
	1	3	5	7
RMS residual, $\mu\text{m}$	1.0925	0.0153	0.0025	0.0014
RMS residual, mas	62.59	0.88	0.15	0.08
Worst central residual, $\mu\text{m}$	2.034	0.040	0.009	0.006
Worst central residual, mas	116.5	2.3	0.5	0.3
Worst corner residual, $\mu\text{m}$	3.841	0.052	0.005	0.003
Worst corner residual, mas	220.1	3.0	0.3	0.2

Using $b_k$	Maximum degree			
	1	3	5	7
RMS residual, $\mu\text{m}$	1.0925	0.0163	0.0030	0.0018
RMS residual, mas	62.59	0.94	0.17	0.10
Worst central residual, $\mu\text{m}$	2.034	0.055	0.010	0.005
Worst central residual, mas	116.5	3.2	0.6	0.3
Worst corner residual, $\mu\text{m}$	3.841	0.043	0.005	0.003
Worst corner residual, mas	220.1	2.5	0.3	0.2



**Fig. 1.** Layout of images in the astrograph focal plane. Points are placed at 0.5-deg intervals from  $-3$  to  $+3$  deg in each coordinate. Filled circles correspond to images actually produced; open circles were derived from symmetry considerations.